Plant Science 332 (2023) 111718

Contents lists available at ScienceDirect

Plant Science

journal homepage: www.elsevier.com/locate/plantsci

Indole-3-acetaldoxime delays root iron-deficiency responses and modify auxin homeostasis in *Medicago truncatula*

Angela Roman [a,1], Joaquín Montenegro [a,1], Laura Fraile [a], Marina Urra [b], Javier Buezo [b], Alfonso Cornejo [c], Jose Fernando Moran [b,2], Yolanda Gogorcena [a,*,3]

[a] *Department of Pomology, Aula Dei Experimental Station, Consejo Superior de Investigaciones Científicas (CSIC), Avda. de Montañana 1005, E-50059 Zaragoza, Spain*
[b] *Institute for Multidisciplinary Research in Applied Biology (IMAB), Department of Sciences, Public University of Navarre (UPNA), Avda. de Pamplona 123, E-31192 Mutilva, Spain*
[c] *Institute for Advanced Materials and Mathematics (INAMAT2), Department of Sciences, Public University of Navarre (UPNA), Campus de Arrosadía, E-31006 Pamplona, Spain*

ARTICLE INFO

Keywords:
Max 6: Iron chlorosis
Ferric-Chelate Reductase
pH-decrease
Flavins
Superroot
IAOx-pathway

ABSTRACT

Iron (Fe) is an essential plant micronutrient, being a major limiting growth factor in calcareous soils. To increase Fe uptake, plants induce lateral roots growth, the expression of a Fe(III)-chelate reductase (FCR), a Fe(II)-transporter and a H^+-ATPase and the secretion of flavins. Furthermore, auxin hormone family is involved in the Fe-deficiency responses but the action mechanism remains elusive. In this work, we evaluated the effect of the auxin-precursor indole-3-acetaldoxime (IAOx) on hydroponically grown *Medicago truncatula* plants under different Fe conditions.

Upon 4-days of Fe starvation, the pH of the nutrient solution decreased, while both the FCR activity and the presence of flavins increased. Exogenous IAOx increased lateral roots growth contributing to superroot phenotype, decreased chlorosis, and delayed up to 3-days the pH-decrease, the FCR-activity increase, and the presence of flavins, compared to Fe-deficient plants. Gene expression levels were in concordance with the physiological responses.

Results: showed that IAOx was immediately transformed to IAN in roots and shoots to maintain auxin homeostasis. IAOx plays an active role in iron homeostasis delaying symptoms and responses in Fe-deficient plants. We may speculate that IAOx or its derivatives remobilize Fe from root cells to alleviate Fe-deficiency. Overall, these results point out that the IAOx-derived phenotype may have advantages to overcome nutritional stresses.

1. Introduction

Iron (Fe) is an essential micronutrient for plants since it takes part in fundamental biological redox processes. Despite Fe abundancy on soils, Fe deficiency by poor availability in calcareous soils is a major nutrient limiting factor that provokes leaf chlorosis and other disorders that reduce crop yield and quality (Lindsay and Schwab, 1982). For instance, it has been estimated that up to 50% of fruit trees in the Mediterranean basin suffer from Fe deficiency (Abadía et al., 2004).

Under Fe starvation conditions, plants develop different strategies for the uptake of Fe from soil. Strategy I is based on the reduction of Fe (III), and includes dicotyledonous and non-Graminaceae monocotyledonous species, whereas Strategy II use a Fe(III) chelation-based mechanism by secretion of phytosiderophores, and includes Graminaceae species (Abadía et al., 2011). To increase the Fe uptake capacity, Strategy I plants display morphological changes such as swelling of root tips and formation of lateral roots and root hairs to increase the root surface (Schmidt, 1999; López-Millán et al., 2000; Müller and Schmidt, 2004). Also biochemical changes increase Fe uptake by the induction of a plasma-membrane Fe(III) chelate-reductase (FCR) (Moog and Brüggemann, 1994), a Fe(II) transporter (Fox and Guerinot, 1998), and a plasma-membrane H^+-ATPase (Santi and Schmidt, 2009). The latter

* Corresponding author.
E-mail address: aoiz@eead.csic.es (Y. Gogorcena).
[1] Contributed equally
[2] ORCID 0000-0001-6621-6961
[3] ORCID 0000-0003-1081-430X

https://doi.org/10.1016/j.plantsci.2023.111718

Available online 25 April 2023

increases proton extrusion lowering soil pH to favor the solubilization of inorganic Fe. Roots also release different compounds including carboxylates, phenolics, and flavins to chelate Fe(III) (Abadía et al., 2002; Jin et al., 2007; Fourcroy et al., 2014; Sisó-Terraza et al., 2016).

Medicago spp. are legume species generally tolerant to Fe-deficiency in calcareous soils (Andaluz et al., 2009; Rodriguez-Celma et al., 2011). Under Fe-deficiency conditions, the model species *Medicago truncatula* displayed a biomass reduction of roots and shoots, a decrease in the length of roots, the number of trifoliate leaves, and chlorophyll levels (Montejano-Ramírez et al., 2020), yellow and swollen root distal regions, and short lateral roots (Andaluz et al., 2009; Rodríguez-Celma et al., 2011). It is also described that Fe-deficient grown *M. truncatula* and *M. scutellata* plants developed other responses in roots such as acidification of the medium, induction of the FCR activity, and production and secretion of riboflavins (Rbfl) as well as other hydroxylated-flavins derivatives (Andaluz et al., 2009; Rodríguez-Celma et al., 2011; Li et al., 2014; Ben Abdallah et al., 2017; Gheshlaghi et al., 2020).

Hormones and small signaling molecules are involved in Fe-deficiency responses, including ethylene (Li et al., 2014; Lucena et al., 2015), auxin (Chen et al., 2010; Jin et al., 2007; Bacaicoa et al., 2011; Jin et al., 2011), cytokinins (Séguéla et al., 2008), abscisic acid (ABA) (Lei et al., 2014), gibberellins (Wild et al., 2016), brassinosteroids (Wang et al., 2019), and signaling molecules like nitric oxide (NO) (Romera and Alcántara, 1994; Graziano and Lamattina, 2007; Jin et al., 2011; Yu et al., 2014). Auxin can stimulate root branching and root hair formation on Fe-deficient plants (Li and Schmidt, 2010). Particularly, indole-3-acetic acid (IAA) has been related to Fe status by both increasing its concentration in Fe-deficient roots (Jin et al., 2007; Bacaicoa et al., 2009) and significantly enhancing the ferric reduction system (Jin et al., 2006). Exogenous application of IAA in several plant species like tomato, cucumber, and *Arabidopsis* induced the expression of Fe-deficient responsive genes including *IRT1* (iron-regulated transporter 1), *FRO2* (ferric reductase oxidase 2), and *AHA* (plasma membrane H^+-ATPase) (Bacaicoa et al., 2011; Hindt and Guerinot, 2012, and references therein).

Interestingly, most of the promoters of Fe response genes contained a large number of ARF (auxin-responses-factors)-binding motifs, which are the molecular bases of auxin regulated Fe deficiency responses (Li et al., 2015; Schwarz et al., 2020). The expression of those Fe responsive genes is regulated by the transcription factor FER-LIKE IRON--DEFICIENCY-INDUCED TRANSCRIPTION FACTOR (FIT1) in *Arabidopsis thaliana* (Colangelo and Guerinot, 2004), which additionally forms heterodimers with the basic helix-loop-helix (bHLH)38 and bHLH39, among other transcription factors (Yuan et al., 2008). It has also been suggested that Rbfl synthesis is under the control of FIT1/bHLH38/bHLH39 heterodimers (Vorwieger et al., 2007). Also, in *M. truncatula* roots, genes involved in the first steps of Rbfl biosynthesis (3,4-dihydroxy-2-butanone-4-phosphate, *MtGTPcII* or 6,7-dimethyl-8-(1D-ribityl)lumazine, *MtDMRL*) and genes encoding plasma membrane transporters for Fe-binding compounds (Hippo-campus Abundant Transcript-Like proteins from the major facilitator transporter superfamily, *MtMFS*), were strongly induced by Fe deficiency (Rodríguez-Celma et al., 2013).

IAA is considered the major auxin in plants, however, a number of additionally occurring compounds and a variety of IAA precursors with auxinic effect have been reported (Mano and Nemoto, 2012; Sánchez-Parra et al., 2014; Tivendale. et al., 2014; Olatunji et al., 2017). The biosynthetic pathways of those compounds still remain elusive, largely because several biosynthesis routes coexist with intermediate steps not yet identified, but also because the enzymes involved show redundant functions. Indole-3-acetaldoxime (IAOx) is an intermediate precursor of the IAOx pathway for tryptophan-dependent auxin biosynthesis (Celenza, 2001; Sugawara et al., 2009). This pathway has been reported as unique to the Brassicaceae family (Sugawara et al., 2009). However, evidence has been found that IAOx can be synthetized in heterologous systems in maize (Irmisch et al., 2015) and also accumulated significantly in the Fabaceae species *M. truncatula* (Buezo et al., 2019). Exogenous IAOx produces a phenotype on *M. truncatula* similar to *SUR*-defective *Arabidopsis* mutants *sur1* and *sur2* (Boerjan et al., 1995), which showed an increase in the number of lateral roots whereas a reduction of the main root elongation was observed (Buezo et al., 2019). However, the mechanisms whereby IAA is produced from IAOx are still unclear in most plant species. IAOx can be either dehydrated to indole-3-acetonitrile (IAN) by an IAOx dehydratase (encoded by *CYP71A13* in *A. thaliana*) (Nafisi et al., 2007) or transformed to indole-3-acetaldehyde (IAAld) (Rajagopal and Larsen, 1972; Tivendale. et al., 2014). In *Arabidopsis*, there is also evidence that IAOx generates indole-3-acetamide (IAM) (Sugawara et al., 2009) but this pathway is not essential to generate IAA (Pérez-Alonso et al., 2021). However, the processes by which IAOx is transformed to IAAld or IAM remains still largely unknown. The three routes can subsequently produce IAA either by a nitrilase (encoded by *NIT1–3* in *Arabidopsis*), a process which is not well understood yet (Bartel and Fink, 1994), or by an indole-3-acetaldehyde oxidase (AO) (Tivendale et al., 2014) or by members of the enzyme family AMIDASE 1 (AMI1), reportedly widespread among plants (Lehmann et al., 2010).

Many studies proved that auxin hormone family is involved in the Fe-deficiency responses (Chen et al., 2010; Jin et al., 2007; Bacaicoa et al., 2011; Jin et al., 2011) but the specific mechanism remains elusive. To shed light, in this work we have evaluated the effect of the auxin precursor IAOx on *M. truncatula* plants grown in hydroponics under different Fe nutrition conditions. We evaluated morphological and physiological traits, and studied transcriptomic changes of paramount genes on the IAOx-IAA pathway in *M. truncatula* in response to the different Fe treatments for 7 days. We mostly focused at the root level since it is the primary organ in charge of Fe uptake. Our results indicate that exogenous IAOx produces a phenotype on hydroponically grown *M. truncatula* plants similar to *SUR*-defective *Arabidopsis* mutants. Up to four days, lateral roots developed intensively, whereas root elongation was reduced in comparison with untreated plants. The increase of the number of secondary roots and density (root hairs) increase the root surface that facilitates the nutrition of macro and micro-elements. Thereby, we hypothesize that exogenous IAOx confers advantages to overcome nutritional deficiencies. Auxin (IAA or its precursors) may have a signaling role to overcome Fe-limited stress conditions.

2. Material and methods

2.1. Plant material, growth conditions and treatments

Seeds of *Medicago truncatula* Gaertn. ecotype Jemalong A17 were scarified with 95% sulphuric acid for 8 min and sterilised with 3% sodium hypochlorite for 5 min. The seeds were germinated on humid filter paper on vertically placed Petri dishes at 14 ºC in a cooled incubator (IPP 200, Peltier-Technology, Memmert, Buchenbach, Germany) in darkness for 6 days (modified from Buezo et al., 2019). Seedlings were transferred to aerated 10 L hydroponic ½ strength Hoagland media pH 5.5 (2.5 mM KNO_3, 1 mM $MgSO_4 \bullet 7H_2O$, 1 mM KH_2PO_4, 0.5 mM NaCl, 2.5 mM $Ca(NO_3)_2 \bullet 4H_2O$, 4.6 μM $MnCl_2 \bullet 4\ H_2O$, 23.2 μM H_3BO_3, 0.06 μM $Na_2MoO_4 \bullet 2H_2O$, 1,2 μM $ZnSO_4 \bullet 7H_2O$, 0.19 μM $CuSO_4 \bullet 5H_2O$, 45 μM NaFe(III)-ethylenediaminetetraacetate [Fe(III)-EDTA], (Rodríguez-Celma et al., 2011) for 4 days. Seedlings in hydroponic media were grown in a bioclimatic chamber (Fitoclima 10.000EHHF, Aralab, Albarraque, Portugal) under controlled conditions (70% of relative humidity, 16 h, 23 ºC / 8 h, 19 ºC day (350 μmol m^{-2} s^{-1}) / night regime).

Seedlings of *M. truncatula* were transferred to aerated 0.5 L pots under control (45 μM NaFe(III)-EDTA) or iron-deficient (0 μM NaFe(III)-EDTA) conditions with or without 100 μM of chemically synthetised IAOx (Buezo et al., 2019) for seven days. IAOx was diluted in dimethyl sulfoxide (DMSO) at a final concentration of 0.25 μL/mL. The same concentration of DMSO was added to plants without hormonal

treatment.

2.2. Assessment of morphological and physiological changes and sampling

Morphological and physiological parameters were recorded every 2–3 days (d) on 3–20 replicates, depending on the parameter. We have monitored: main root length, number of lateral roots, shoot area, root and shoot fresh weight (FW) also called biomass, pH of the culture media, and recorded the yellow coloration (typical of the presence of flavins) in the root tips (Weinstein et al., 1954) or in the media (Pound et al., 1958). Morphological measurements, as lateral root number and the shoot area were analysed with ImageJ software.

The iron chlorosis level was assessed with a SPAD-502 Chlorophyll Meter (Minolta Camera Co., Osaka, Japan) in individual first leaf and in young trifolium when the area fit the window that allows reading. Three measurements were taken per plant and, at least, three replicates per treatment, in at least three experiments.

The ferric-chelate reductase (FCR) activity was measured in vitro according to methodology previously described (Gogorcena et al., 2000; Jiménez et al., 2008) adapted to *M. truncatula* plants. Briefly, in vitro measurements were performed in 1.5 mL microtubes containing whole root (~ 50–80 mg) of one *M. truncatula* plant. Roots were rinsed in deionised water and introduced into 950 μL of 10 mM MES pH 6, 0.3 mM bathophenanthroline disodium salt (BPDS, ACROS Organics, Geel, Belgium) and 50 μL Fe(III)-EDTA (Sigma, St. Louis, MI, USA) of 10 mM to a final concentration of 0.5 mM. The reaction was performed for ~ 45 min in darkness at room temperature. Aliquots of 0.5 mL were taken and absorbance was measured at 535 nm in a spectrophotometer (UV-2450, Shimadzu, Tokio, Japan). Reduction rates of Fe(III) were estimated from the formation of Fe(II)-$BPDS_3$ coloured complex and an extinction coefficient of 22.14 mM^{-1} cm^{-1}. For each treatment, 4–8 replicates were used.

Morphological changes in roots and the yellow coloration asociated to the presence of flavins were imaged with a binocular stereoscope (Nikon SMZ745T, Derby, UK). Images were recorded by digital camera (Nikon Digital sight DS-Fi1) and processed using NIS-Elements F 4.60.00 (Nikon). Visualization of fluorescent flavin compounds on roots was performed using a UV transilluminator (Gel Doc 2000, Bio-Rad, Hercules, CA, USA) at 302 nm excitation wavelength and 1–2 s of exposure time using the Quantity One® analysis software (version 4.6.9, BioRad).

Nutrient solution, and root and leaf samples were collected at times 0 h, 2 h, 2 d, 4 d, and 7 d for metabolic or transcriptomic analysis. Plant samples were weighted and immediately frozen in liquid N_2 and stored at − 80 °C until they were analysed.

2.3. Synthesis of indolic compounds and the determination of its content in plant tissues

1*H*-Indole-3-acetaldehyde (IAAld) was produced by chemical synthesis from tryptophan and used as a reactant to produce IAOx, which was synthesised and its purity checked as described in Buezo et al. (2019).

The contents of auxin and indolic compounds IAA, IAOx, IAN and IAM were determined in roots and shoots by HPLC-fluorescence as described in Buezo et al. (2019). The extraction methodology was adapted from that reported by Esteban et al. (2016). Approximately 200 mg of frozen plant tissue were ground to powder in a mortar with liquid N_2 and then homogenized with 5 mL of a solution of Methanol:H_2O (80:20, v/v) stabilized with BHT (200 mg·L^{-1}), there upon transferred to a 50 mL centrifuge tube adding 1*H*-Indole-3-propanoic acid as the internal standard (see details for further procedure in Buezo et al. (2019). For each treatment, 3–5 replicates were used.

HPLC coupled to a fluorescence detector was performed using Waters 575 HPLC Pumps (Waters, Milford, MA, USA) controlled by a Waters Pump Control Module (Waters) and a Waters 474 fluorescence detector (Waters) using a μBondapak C18 column (10 μm 125 Å 3.9 ×150 mm, WAT86684 Waters) with a mobile phase of solvent A (water with 0.4% v/v acetic acid) and B (acetonitrile), with a constant flux of 0.5 mL per min. A gradient-increasing concentration was used for solvent B, from 20% to 40% during 25 min and then held during 10 min. The concentration of B was then gradually decreased to 20% during 5 min and held for 5 min. Fluorescence detector was set at λ_{ex}= 280 nm λ_{em}= 331 nm with a gain of 10. Standards of IAM, IAA, IAOx and IAN were used to determine retention times and concentration calibration. Retention times were 6.70 min for IAM, 10.17 min for IAA, 13.17 min for the first isomer of IAOx, 13.55 min for the second isomer of IAOx, 13.81 min for the internal standard (indole-3-propanoic acid) and 15.03 min for IAN.

2.4. RNA extraction and Reverse Transcription (RT)-qPCR

Roots samples (100 mg) from at least 3 replicates of each treatment from at least 3 independent experiments were ground to a fine powder in a bead-beater mill (MM400, Retsch, Haan, Germany) with liquid nitrogen before extraction. RNA extraction was performed using AMBION® RNAqueous isolation kit (Thermo Fisher Scientific, Waltham, MA, USA) and AMBION® Plant RNA Isolation Aid (Thermo Fisher Scientific) reactive following manufactures instructions. RNA was quantified in a NanoDrop 2000 spectrophotometer (Thermo Fisher Scientific) and the integrity of RNA was checked by electrophoresis. Subsequently, samples were treated with DNase I (Thermo Fisher Scientific). One μg of total RNA was reverse transcribed using oligo (dT)18 as a primer with RevertAid H Minus First Strand cDNA Synthesis Kit (Thermo Fisher Scientific). The qPCR reactions were performed with two technical replicates of 20 μL (15 ng cDNA, 10 μL of SybrGreen (KAPA, Sybr FastROX, Sigma), 0.2 μM primers) in a QuantStudio 3 thermocycler (Thermo Fisher Scientific). The qPCR program was: 95 °C for 10 min, 40 cycles of 15 s at 94 °C followed by 1 min at 60 °C, and a final melting curve was programmed to confirm the absence of contamination or unspecific amplification in all samples. qPCR reaction efficiencies were determined for each primer pair using LinRegPCR software (Ruijter et al., 2009) and the transcript levels were determined using mean (qPCR efficiency)-Ct relative to the geometric mean (qPCR efficiency)-Ct (Vandesompele et al., 2002) of the two reference genes *actin-11* (*Medtr7g026230*) and *26S proteasome regulatory subunit S5A_2* (*Medtr5g022440*). Primer sequences for *M. truncatula* are listed in Table 1. Some primers were already published and others were designed using Primer3web software (https://primer3.ut.ee/) and their quality was verified using NetPrimer software (http://www.premierbiosoft.com/netprimer/).

2.5. Statistical analysis

Graphs show a representative experiment among at least 3 independent experiments, values are mean ± standard error (SE) of n = 3–20 replications depending on the parameter. Differences between treatments were tested with Student t-test. The resulting *P* values were considered statistically significant at $\alpha < 0.05$. Different superscripted letters represent statistically significant differences at $\alpha = 0.05$ after Student-Newman-Keuls test.

3. Results

3.1. Morphological and physiological changes

Figs. 1–3 show the main morphological and physiological changes found in plants treated during seven days. We describe changes, first after iron starvation and after IAOx addition in shoots, then in roots.

The general physiological status of the plants of *M. truncatula* transferred to control (45 μM NaFe(III)-EDTA) or iron starvation conditions (0 μM NaFe(III)-EDTA) was monitored during 7 days. Fe-deficient plants developed several symptoms associated with the limitation of Fe content. Those plants displayed a decrease in shoot area

Table 1
Primer sequences for *M. truncatula* RT-qPCR experiments designed in this work or obtained from the cited reference.

Primer name	Gene ID	Primer sequence	Reference
MtFIT_F	*Medtr4g057270*	GCATTGCGTTCTTTGGTTCC	(Montejano-Ramírez et al., 2020)
MtFIT_R		GTCCTGCAACCTCAGCCTTA	
MtAHA5_F	*Medtr2g036650*	ATTCCTATTGCTATGCCAACTG	(Damiani et al., 2016)
MtAHA5_R		ATCAACACCCTTTACAAACACC	
MtFRO2_F	*Medtr8g028795*	TGGCTCAAGATAAAGTGAAAAGG	This work
MtFRO2_R		AACCCAGAAACAGTAACACCA	
MtIRT1_F	*Medtr4g083570*	TGAAAGTGACGAGCCACAAC	This work
MtIRT1_R		CATTTGATGGAAGCACATGG	
MtbHLH39_F	*Medtr7g090410*	GCATTCTGCCCACCTCAGTT	(Montejano-Ramírez et al., 2020)
MtbHLH39_R		TGGTGAAGAGAATTGATGATACGG	
MtGTPcII_F	*Medtr2g009270*	TCTGGTAGGATCCCGTTGTT	(Rodríguez-Celma et al., 2011)
MtGTPcII_R		CCCATTTTCGTACGTTTGGT	
MtDMRLs_F	*Medtr4g094700*	ATCATCATCCCCAACATCGT	(Rodríguez-Celma et al., 2011)
MtDMRLs_R		AGTGGCGGTTTTAGGAGCTT	
MtMFS_F	*Medtr1g092870*	GCGATGCTCCCTTTGAATGC	This work
MtMFS_R		GCCCTCCAAGTCATCATCCC	
MtCyp71A_F	*Medtr4g104540*	AAAGGCTCTACTACTGGACATG	This work
MtCyp71A_R		GTTCTACCATTAGCCACTCTC	
MtAO_F	*Medtr5g087410*	TCAATGCATTATTTGTGACACTTGT	This work
MtAO_R		TCCATTCCATACAGCCTTTCCT	
MtNIT4-like_F	*Medtr4g052390*	ATCCGGTTACTTTTGCCTCG	This work
MtNIT4-like_R		AGGTTTGGAAGTTGCTGACCA	
MtAMI1_F	*Medtr1g082750*	CTGATTGGGCAAGGACTCAT	This work
MtAMI1_R		CCAGGTACTCGGTCTTCTGC	
Mtactin_F	*Medtr7g026230*	CCTAAGGCCAATCGTGAGAA	(Rodríguez-Celma et al., 2011)
Mtactin_R		AAAGAACGGCCTGAATAGCA	
MtProtS5A_F	*Medtr5g022440*	TGGCAGGAAAGGGTGTTC	(Larrainzar et al., 2015)
MtProtS5A_R		GCCACCTGAATACCAGCAG	

FIT (transcription factor *FER-LIKE IRON DEFICIENCY-INDUCED*), *AHA5* (plasma membrane H^+-ATPase), *FRO2* (Ferric reductase oxidase 2), *IRT1* (iron-regulated transporter 1), *bHLH39* (transcription factor ORG2), *GTPcII* (GTP cyclohydrolase II), *DMRLs* (6,7-dimethyl-8-ribityllumazine synthase), *MFS* (Hippocampus abundant transcript-like protein from the major facilitator transporter superfamily), *Cyp71A* (cytochrome P450 family 71A13), *AO* (indole-3-acetaldehyde oxidase), *NIT4-like* (nitrilase/nitrile hydratase NIT4A-like protein), *AMI1* (amidase 1), actin (actin-11) and *ProtS5A* (26S proteasome regulatory subunit S5A_2).

(Fig. 1 A-B), biomass (FW) (Fig. 1 C), and SPAD values, which indicate an increase in leaf chlorosis. Chlorosis was observed both in the first individual leaf and in the young trifoliate leaves (Fig. 1 D-E).

Chemically synthesised IAOx was externally applied to the Fe-sufficient or Fe-deficient hydroponics media of *M. truncatula*. The chosen concentration was 100 μM as it was previously tested on *M. truncatula* grown in vitro (Buezo et al., 2019) and because IAOx in nutrient solution degrades upon time and under light exposure (Supp Fig. 2). A unique dose of 100 μM of IAOx was able to induce changes in the phenotype from day 4. The shoots of Fe-sufficient plants treated with IAOx were significantly smaller than the control plants (shoot area and biomass) (Fig. 1 A-C). The shoots of plants under both Fe-deficiency and IAOx treatments had the same size and biomass as Fe-sufficient plants treated with IAOx (Fig. 1 A-C). However, these plants had lower biomass from day 4 of treatment when compared to Fe-deficient plants (Fig. 1 C), but surprisingly they were not as chlorotic as the latter until day 7 (Fig. 1 D-E).

Changes were observed also in roots from day 4 of Fe-deficient conditions (Fig. 2). Fe starvation led to a decrease in root length (Fig. 2 A-B) and biomass (FW) in 4 days-treated plants (Supp Fig. 1), and to an increase in the number of lateral roots and root hairs (Fig. 2 A, F). At day 7 of Fe-deficient conditions, root length, root weight, and its ratio (weight/length) were significantly lower than control plants, which indicated major decreases in root weight compared to root length (Fig. 2 C and Fig S1).

IAOx addition also induced superroot phenotype in *M. truncatula* plants: total inhibition of the main root growth (Fig. 2 A-B) and an increase in the number of lateral roots (Fig. 2 A, D, E, G). Roots from plants treated with IAOx were shorter and displayed lower biomass (FW) but they were thicker than untreated plants, as the weight/length (g cm^{-1}) ratio of roots was significantly higher (Fig. 2 C). Plants under both Fe-deficiency and IAOx treatments presented a total inhibition of the main root growth (Fig. 2 A-B), an increase in the number of short lateral roots (Fig. 2 A and E) and a decrease in the root biomass, similar to the Fe-deficient plants (Supp Fig. 1). The weight/length ratio of roots was higher than Fe-deficient plants but lower than the control plants treated with IAOx at day 7 (Fig. 2 C).

The initial pH of the nutrient solution was 5.5 and it was monitored daily. The pH increased in the medium of the control plants at a rate of 0.16 units per day to a final value of 6.6, while in the Fe-deficient solution the pH decreased from day 3–4 of treatment from pH 5.5 to levels of pH ~ 4.3 (Fig. 3 A). The FCR activity was assayed in vitro at days 4 and 7 upon iron starvation. Fe-deficient treated plants displayed an increase in the reductase activity compared to sufficient plants (about 5 and 3-fold, respectively) (Fig. 3 B-C).

The presence of a yellow coloration related to flavins inside the root tips and their release into the media were visually monitored. Only Fe-deficient plants exhibited yellow root tips due to flavins production, from day 4 upon treatment. By stereomicroscopy, it appears that flavins were located in the subapical region of lateral roots (Fig. 3 D) and in the main root. Due to the fluorescent properties of flavin compounds, roots were also imaged by UV transillumination at days 4 and 7 upon iron starvation (Fig. 3 E-F). The nutrient solution also exhibited a yellowish coloration under Fe starvation, due to flavins secretion from roots to the nutrient medium (data not shown).

IAOx addition delayed the increase in the pH of the media in control conditions (Fig. 3 A) and the FCR activity of IAOx-treated plants was similar at day 4 but lower at day 7 compared with non-treated plants (Fig. 3 B-C). In the same way, plants under both Fe-deficiency stress and IAOx treatment presented a delay in the pH decrease (Fig. 3 A) until day 7 of treatment, and fluorescence (Fig. 3 E-F) suggest that the apparition of flavins in root tips or secreted to the nutrient solution was also delayed up to 3 days with respect to the Fe-deficient plants. Similarly, in plants under both treatments the Fe reductase activity increased significantly at day 7 compared to sufficient or deficient plants (about 8 and 2.6-fold, respectively).

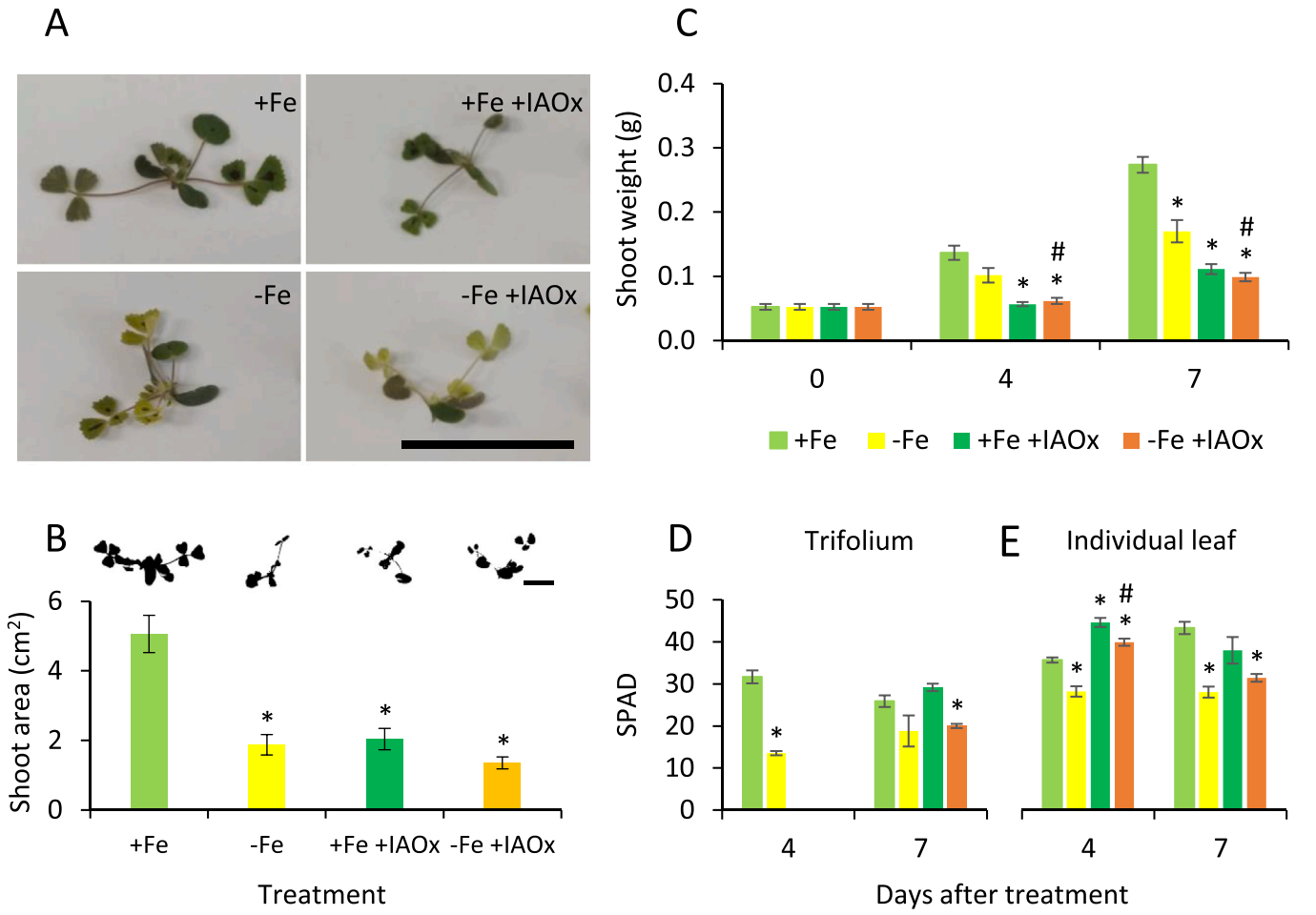

Fig. 1. Morphological and physiological changes in shoots of *M. truncatula*. (A) Visual appearance of 7 days old *M. truncatula* shoots treated with or without Fe and with or without IAOx (+Fe, -Fe, +Fe +IAOx, -Fe +IAOx), bar scale 5 cm. (B) Area of shoots at 7 d, bar scale 2 cm, (C) Weight (g of FW) of shoots and (D-E) SPAD values in young trifolium leaves and the individual leaf. Values represent mean ± SE of 3–12 replicates. Asterisks (*) indicate significant differences among each treatment with respect to the control plants (+Fe) and hash symbols (#) differences between Fe-deficient plants treated with IAOx (-Fe +IAOx) with respect to Fe-deficient plants (-Fe) calculated using Student's test ($P < 0.05$). At day 4, trifolium leaves of IAOx treated plants were very small for SPAD measures.

3.2. Hormone content

We evaluated the hormone (IAOx, IAN, IAM, and IAA) content in roots and shoots in order to verify whether the exogenous IAOx was uptaken by roots and assimilated or transformed into the plant. The hormone content was evaluated by HPLC-fluorescence, at day 0 of treatment (Fig. 4 A) and 4 days after IAOx treatment (Fig. 4 B-E). We found that endogenous IAOx accumulates in high amounts in shoots and roots (83 and 71.2 ng g^{-1} (FW), respectively, Fig. 4 A) in control conditions (+Fe day 0).

After 4 days of treatment imposition, no differences were found in the content of hormones in any organ between (+Fe) or (-Fe) plants except for the increase of IAM content in roots of deficient plants (Fig. 4 B-E). IAOx was accumulated only in shoots of plants under both Fe-deficiency and IAOx treatments (Fig. 4 B). Surprisingly, in IAOx treated plants, an important decrease of IAOx levels was found in roots (with or without Fe supply) (Fig. 4 B). Furthermore, in IAOx treated plants, an important increase of IAN levels was found in shoots (with or without Fe supply) (Fig. 4 C) and in Fe-deficient roots. No significant differences were found in IAA levels after IAOx addition (Fig. 4 E).

3.3. Gene expression

In order to understand the regulation of the physiological and biochemical changes observed in treated plants we have studied the expression of key genes. Time course (0 h, 2 h, 2 d, 4 d, and 7 d) RT-qPCR experiments were performed. Althought morphological and physiological changes were not observed before 4 days, we included the time points 2 h and 2 d in the RT-qPCR experiments to observe early expression changes based on the literature. It has been published before that compounds from the IAA pathway induced very early transcriptional changes (Buezo et al., 2019) and Fe-deficiency induced changes in Fe-related genes after 48 h upon treatment (Montejano-Ramírez et al., 2020).

We evaluated the expression of iron metabolism genes including a ferric reductase oxidase (*FRO2),* an iron-regulated transporter (*IRT1)* and a plasma membrane H^+-ATPase (*AHA5*). We also evaluated the expression of genes related to flavin synthesis (*GTPcII* and *DMRL*) and the candidate of root flavin secretion (*MFS*). Two transcription factors (*FIT* and *bHLH39*), which have been described to control the expression of all the former genes (Colangelo and Guerinot, 2004; Yuan et al., 2008), were also included (see Fig. 5).

The release of the *M. truncatula* genome (Mt4.0v1) is relatively recent and the nomenclature of those genes may be confusing among different published studies, especially considering the use of different versions of the genome. *M. truncatula* gene IDs and sequences used in this study have been obtained and updated from *Phytozome v12.1 (primer names and gene IDs are listed* in Table 1). Some of the *M. truncatula* gene IDs used in this study have been previously described in literature and their primers were available (see references in Table 1. Other IDs (*MtMSF*,

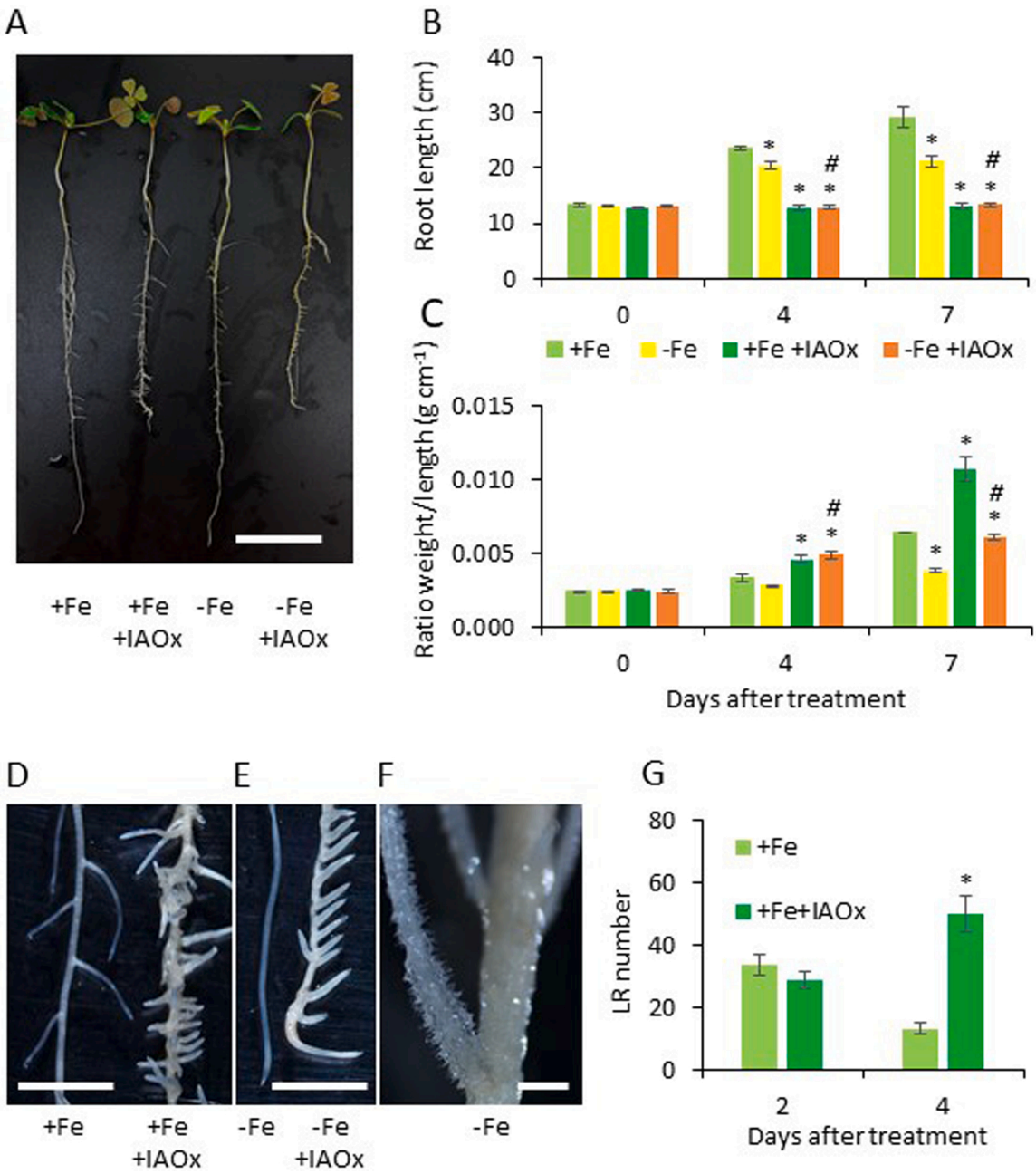

Fig. 2. Morphological changes in roots of *M. truncatula.* (A) Visual appearance of 4 days old *M. truncatula* roots grown with or without Fe and with or without IAOx (+Fe, -Fe, +Fe +IAOx, -Fe +IAOx), bar scale 5 cm. (B) Length of main root, values represent mean ± SE, n = 6–20, and (C) weight / length ratio of roots, values represent mean ± SE, n = 20 (day 0) and n = 3–5 (days 4 and 7). (D) Lateral roots and (E) root tips of *M. truncatula* grown four days under different treatments imaged by stereomicroscopy, scale bar in both 5 mm. (F) Root hairs of Fe-deficient roots imaged by stereomicroscopy, scale bar 1 mm. (G) Number of lateral roots, values represent mean ± SE, n = 4. Asterisks (*) indicate significant differences with respect to the control plants (+Fe) and hash symbols (#) differences between Fe-deficient plants treated with IAOx (-Fe +IAOx) with respect to Fe-deficient plants (-Fe) calculated using Student's test ($P < 0.05$). At day 7, root development was incompatible to counting lateral roots.

MtCyp71A, *MtAO*, and *MtAMI1*) were cited in literature but their primers were designed in this work based on the sequence obtained from the genome version Mt4.0v1. The remaining *M. truncatula* gene IDs (*MtFRO2, MtIRT1,* and *MtNIT4-like*) have been found in this work by homology with their *A. thaliana* orthologues from *The Arabidopsis Information Resource (TAIR11)*.

We first evaluated the expression of key genes in the iron uptake at different times (0 h, 2 h, 2 d, 4 d, and 7 d) of the experiment. An important increase in the expression of all Fe-related genes (*AHA5, FRO2, IRT1,* x17, x45 and x8-fold change compared to control, respectively) and the transcription factors (*FIT, bHLH39,* x4-fold change) controlling those genes in Fe-deficient plants was observed at day 4 (Fig. 6 A-E, Supp Table 1). Next, we evaluated the expression of key genes in flavin synthesis and secretion by roots (*GTPcII, DMRLs,* and *MFS*). Similarly, a dramatic significant increase in the expression of those genes (x84, x58 and x52-fold change, respectively) in Fe-deficient plants was observed at day 4 (Fig. 6 F-H, Supp Table 1).

On the contrary, the expression of genes related to iron or flavins (*FIT, AHA5, FRO2, IRT1, bHLH39, GTPcII, DMRLs,* and *MFS*) diminished in Fe-deficient plants treated with IAOx, in most cases from day 2 after the onset of treatment, with respect to Fe-deficient plants (Fig. 6, Supp Table 1).

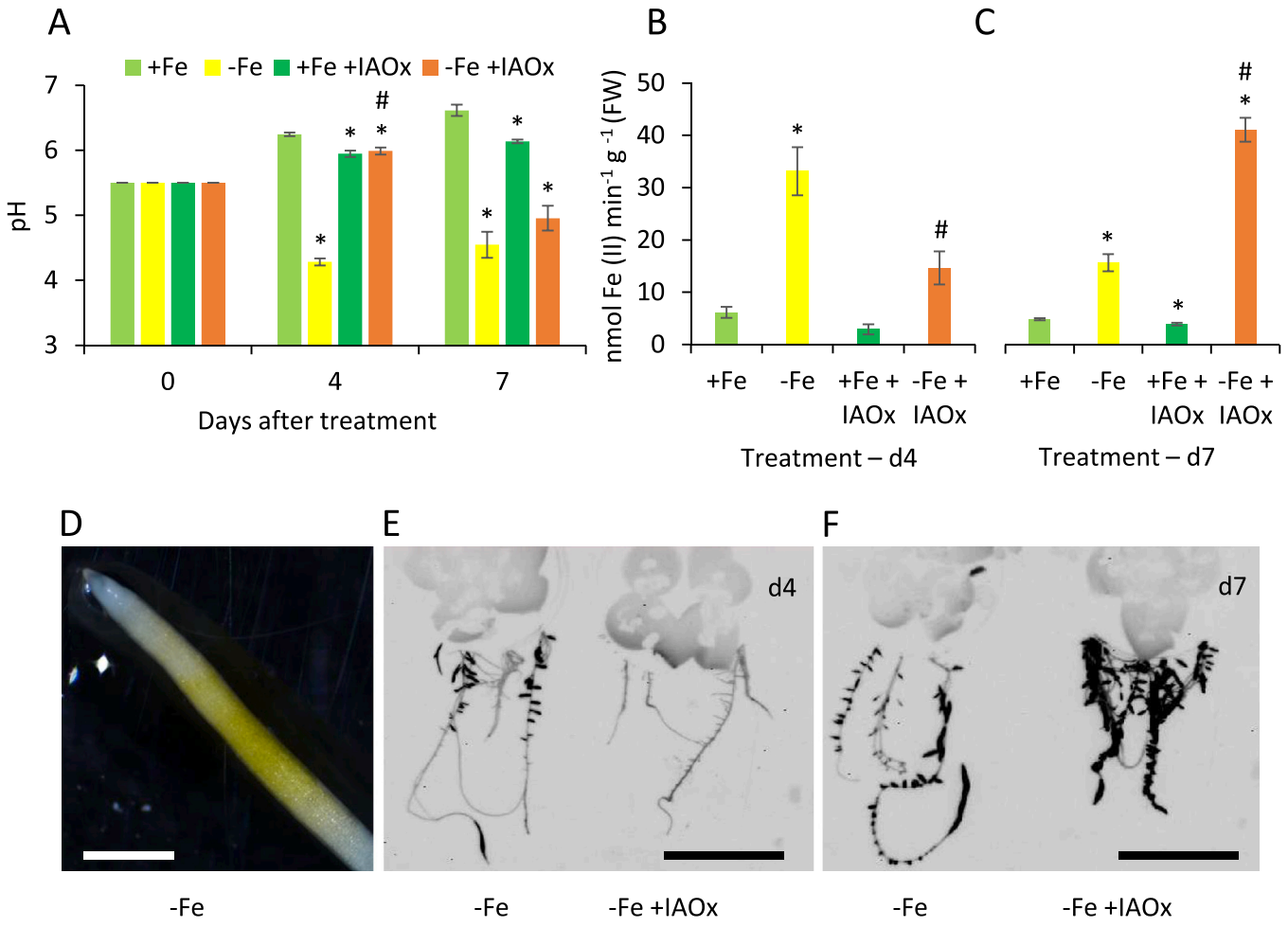

Fig. 3. Physiological responses associated with Fe deficiency (pH, FCR activity and flavins). (A) Changes in pH of nutrient media, values represent mean ± SE, n = 3–5 and (B and C) Ferric-chelate reductase activity of *Medicago* plants treated with or without Fe and with or without IAOx (+Fe, -Fe, +Fe +IAOx, -Fe +IAOx) during 4 or 7 days, values represent mean ± SE, n = 4–8. (D) Fe-deficient root tips showing a yellow coloration related to flavins at day 7 imaged by stereomicroscopy, scale bar 1 mm. (E and F) Fluorescent inverted image of roots showing fluorescent compounds (mainly flavins) (in black obtained by UV transillumination, scale bar 5 cm). It appears at day 4 there was little endogenous induction of flavins (-Fe) or not induction (-Fe +IAOx); while at day 7 there was a strong induction in both (-Fe) and (-Fe +IAOx) treatments. Asterisks (*) indicate significant differences with respect to the control plants (+Fe -IAOx) and hash symbols (#) differences between Fe-deficient plants treated with IAOx (-Fe +IAOx) with respect to Fe-deficient plants (-Fe) calculated using Student's test ($P < 0.05$).

After 7 days of treatments, the expression of some genes (*IRT1, bHLH, GTPcII, DMRLs*) did not display any significant difference among treatments (Supp Table 1). On the other hand, the expression of *FIT, AHA5* and *FRO2* and *MFS* were overexpressed in plants under both nutritional and hormonal treatment (-Fe +IAOx) with respect to control plants (Fig. 7, Supp Table 1) or even to Fe-deficient plants (*FIT*, *AHA5*) (Fig. 7 A-B, Supp Table 1).

In order to integrate hormonal changes and shed light on the IAOx pathway, we studied the expression of known genes involved in the IAA synthesis. As it is stated in the introduction, the metabolite IAOx can be dehydrated to IAN by IAOx dehydratase (Nafisi et al., 2007), or transformed to IAAld or to IAM by processes still to be demonstrated (Tivendale et al., 2014; Olatunji et al., 2017). The three intermediates can subsequently produce IAA, either by a nitrilase (Bartel and Fink, 1994), by AO or by AMI1 (Tivendale et al., 2014), respectively (Fig. 8 A). The expression of the genes (*Cyp71A13, AO, AMI1,*) implicated in these routes in *Medicago* have been evaluated. *NIT1–3* has not been described in *M. truncatula* but, we identified a *NIT4*-like by homology with the *Arabidopsis AtNIT1–4* sequences (identity 68–76%). NIT4 is implicated in the cyanide detoxification pathway but in other species, like maize, nitrilases have been found to perform a dual role in auxin homeostasis and beta-cyanoalanine hydrolysis (Kriechbaumer et al., 2007). Thus, we decided to study *MtNIT4-like* expression too, to test if it could be implicated in IAN transformation to IAA.

As indicated above for the expression analysis, we mostly focused at the root level since it is the primary organ in charge of Fe uptake and most of the genes evaluated (*FIT, AHA5, FRO2, IRT1, GTPcII, DMRLs, MFS)* are essential part of the Fe uptake mechanisms of the roots. In the case of the IAA synthesis related genes (*Cyp71A13, NIT4-like, AO* and *AMI1*) we present expression data only in roots although we have found similar expression profiles in both shoots and roots (data not shown). Results were also consistent with published results in seedlings (Buezo et al., 2019).

In plants treated with IAOx, *Cyp71A*13 expression was highly induced after 2 h of treatment in control-treated or deficient plants (x20 to x25-fold change respect to their control, Fig. 8 B, Supp Table 1). This increase continued over time, especially on Fe-deficient plants treated with IAOx. In contrast, the expression of *NIT4-like, AMI1,* and *AO* were insensitive to the addition of IAOx (Fig. 8 C-E, Supp Table 1).

4. Discussion

Medicago truncatula, as a model plant, has been grown under different conditions in literature. Solid Farhaeus media has been widely used in the in vitro-culture of *M. truncatula* (Esteban et al., 2016; Buezo et al., 2019). However, the complete Farhaeus solution in hydroponic

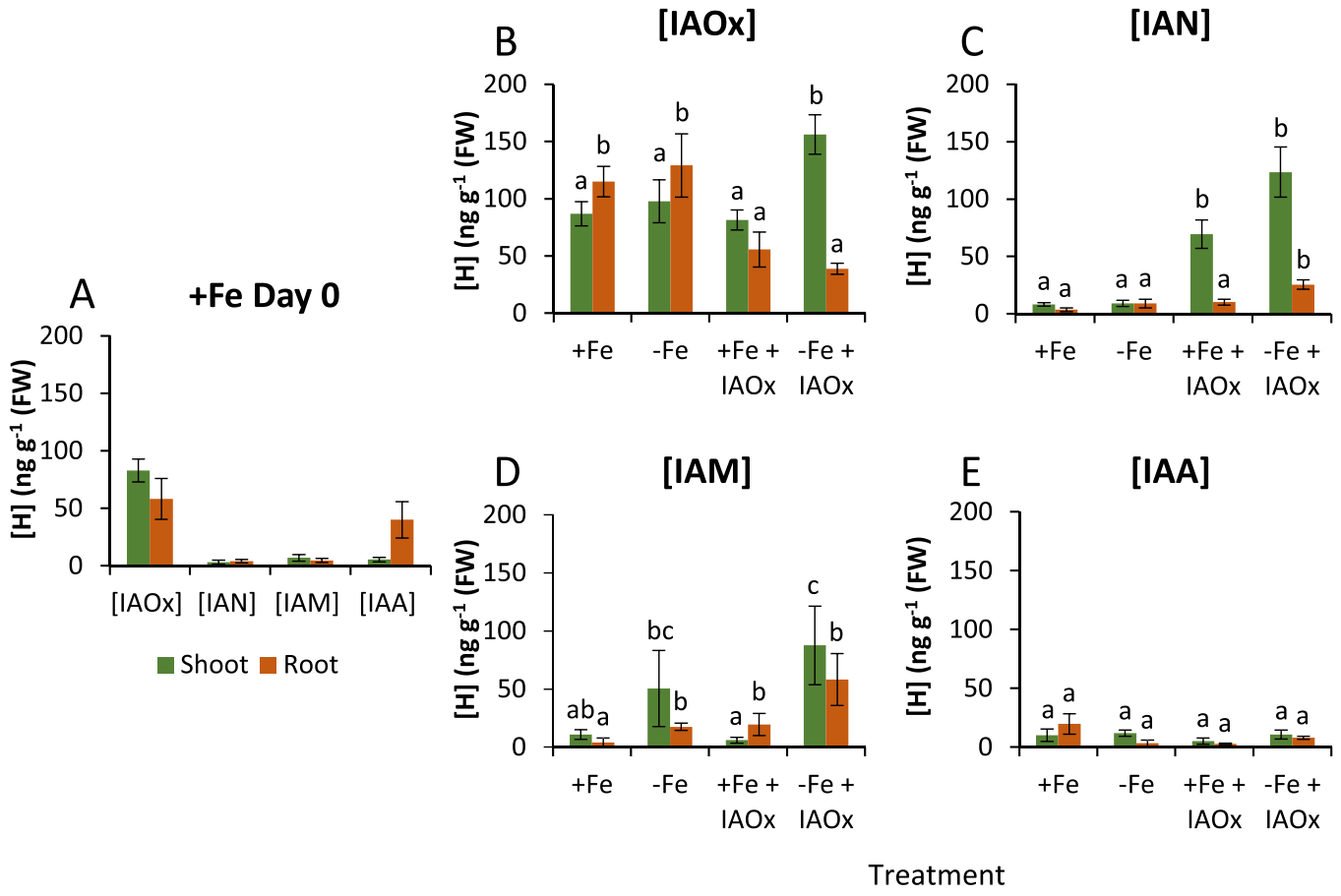

Fig. 4. Endogenous indolic compounds contents (ng g^{-1} (FW)) in *Medicago truncatula* seedlings. (A) IAOx, IAN, IAM and IAA in *Medicago* plants at day 0 in control plants. (B-E) IAOx, IAN, IAM and IAA in *Medicago* plants treated with or without Fe and with or without IAOx (+Fe, -Fe, +Fe +IAOx, -Fe +IAOx) at day 4. Values represent mean ± SE, n = 3–5. In each organ, different superscripted letters represent statistically significant differences after Student-Newman-Keuls test ($P < 0.05$).

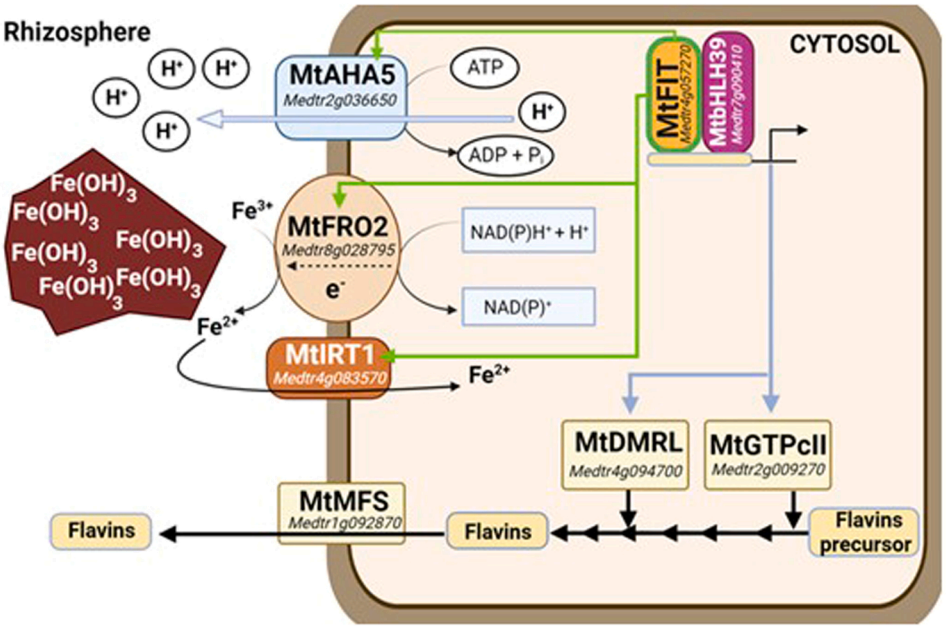

Fig. 5. Schematic representation of the proteins, genes and transcription factors related to iron reduction and transport and to flavin synthesis and secretion in root cells of Strategy I plants. FIT (transcription factor FER-LIKE IRON DEFICIENCY-INDUCED), AHA5 (plasma membrane H+-ATPase), FRO2 (Ferric reduction oxidase 2), IRT1 (Iron-regulated transporter 1), bHLH39 (transcription factor ORG2), GTPcII (GTP cyclohydrolase II), DMRLs (6,7-dimethyl-8-ribityllumazine synthase), MFS (Hippocampus abundant transcript-like protein, major facilitator superfamily).
Adapted from Rodríguez-Celma et al., 2013. Created with BioRender.com.

culture provoked Fe-deficient symptoms (leaf chlorosis or even a decrease in the pH of the media) in control plants. In other studies, *M. truncatula* plants were hydroponically grown with Fe-EDDHA pH 7.5 (Gheshlaghi et al., 2020). Under those latter conditions, plants displayed a high growth rate masking both the IAOx phenotype and the decrease in pH in the buffered-nutrient solution, being pH critical for the onset of

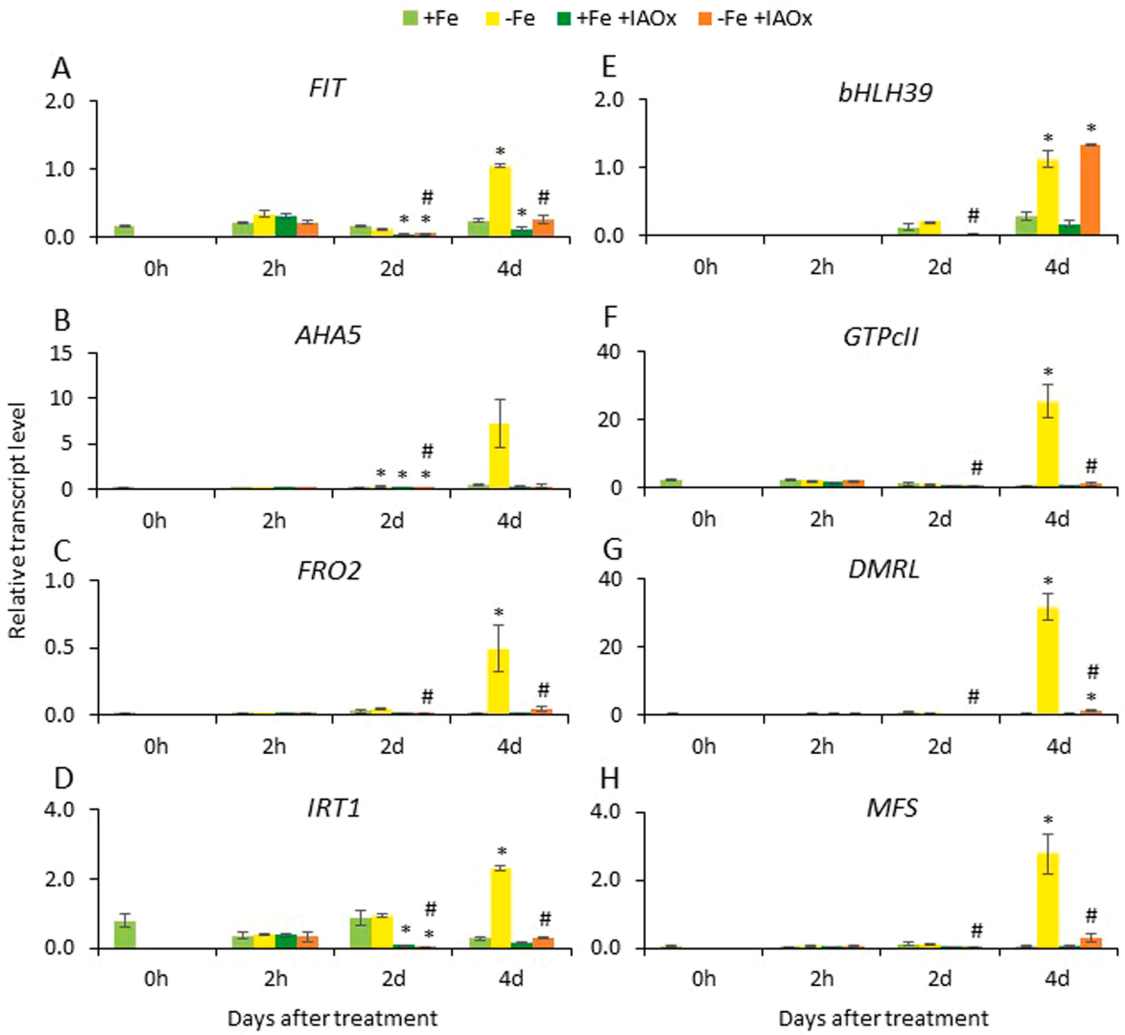

Fig. 6. Relative expression level of genes related to iron reduction and transport and to flavin synthesis and secretion in roots. Time course (0 h, 2 h, 2 d and 4 d) after treatment application (+Fe, -Fe, +Fe +IAOx, -Fe +IAOx). *FIT* (transcription factor FER-LIKE IRON DEFICIENCY-INDUCED*), AHA*5 (Plasma membrane H+-ATPase), *FRO2* (Ferric reduction oxidase 2), *IRT1* (Iron-regulated transporter 1), *bHLH39* (transcription factor ORG2), *GTPcII* (GTP cyclohydrolase II), *DMRLs* (6,7-dimethyl-8-ribityllumazine synthase), *MFS* (Hippocampus abundant transcript-like protein, major facilitator superfamily*)*. Values represent mean ± SE of relative expression to reference genes *actin* (Actin-11) and *ProtS5A* (26S proteasome regulatory subunit S5A_2). Asterisks (*) indicate significant differences with respect to the control plants (+Fe) and hash symbols (#) differences between Fe-deficient plants treated with IAOx (-Fe +IAOx) with respect to Fe-deficient plants (-Fe) calculated using Student's test ($P < 0.05$).

the transcriptomic response of key genes (Tsai and Schmidt, 2020).

In our experimental conditions (Fe(III)-EDTA pH 5.5), Fe-deficient plants developed several symptoms associated with the limitation of Fe content such as leaf chlorosis, decrease in the area and the biomass of shoots and roots, and the increase in the number of lateral roots (Figs. 1 and 2), which increase the root surface in contact with the medium. These morphological changes are in agreement with previously reported results for *M. truncatula* plants upon Fe limitation (Andaluz et al., 2009; Rodríguez-Celma et al., 2013; Gheshlaghi et al., 2020; Montejano-Ramírez et al., 2020).

As well, the acidification of the nutrient solution (Fig. 3 A) is a known mechanism of the Fe-deficient Strategy I plants to favor the solubilization of inorganic Fe, thus increasing its availability in the growth media as illustrated in Fig. 5 (Susín et al., 1993; Santi and Schmidt, 2009; Andaluz et al., 2009; Rodríguez-Celma et al., 2011). In our conditions, the decrease in pH indicated that Fe-deficient plants excreted 1105 nmols of H^+ plant^{-1} day^{-1}. Fe-deficient plants displayed an increase in the reductase activity at any time studied (Fig. 3 B-C) to increase Fe uptake as other studies reported (Moog and Brüggemann, 1994; Jin et al., 2011).

In our experimental conditions, a significant increase in the expression of all Fe-related genes in Fe-deficient plants was observed at day 2–4 (*FIT, AHA5, FRO2, IRT1, bHLH39,* Fig. 6 A-E, Supp Table 1) and at day 7 at a lesser extent (Fig. 7, Supp Table 1), which is in concordance with previously described results in *M. truncatula* (Rodríguez-Celma et al., 2013; Montejano-Ramírez et al., 2020). The gene expression levels are in concordance with the physiological results obtained in this study: a decrease in the pH of the nutrient solution and the increase in the reductase activity observed in Fe-deficient treatments (Fig. 3).

The presence of flavins in the root tips (Fig. 3 D-F) or in the media has been previously reported in several species. Strategy I plants, such as sugar beet or *Medicago,* are capable of releasing different riboflavins (Rbfl and three Rbfl derivatives, 7-OH-Rbfl, 7-COOH-Rbfl and 7α-OH-Rbfl) from the roots to chelate Fe(III) from the media (Sisó-Terraza et al., 2016; Ben Abdallah et al., 2017; Gheshlaghi et al., 2020). In this study, a significant increase in the expression of genes of flavin synthesis and secretion in Fe-deficient plant roots was observed at day 4 (*GTPcII, DMRL and MSF,* Fig. 6, Supp Table 1). This is in concordance with the observed yellow coloration and fluorescent signal (related to flavins apparition) in Fe-deficient plant roots and nutrient solution at day 4

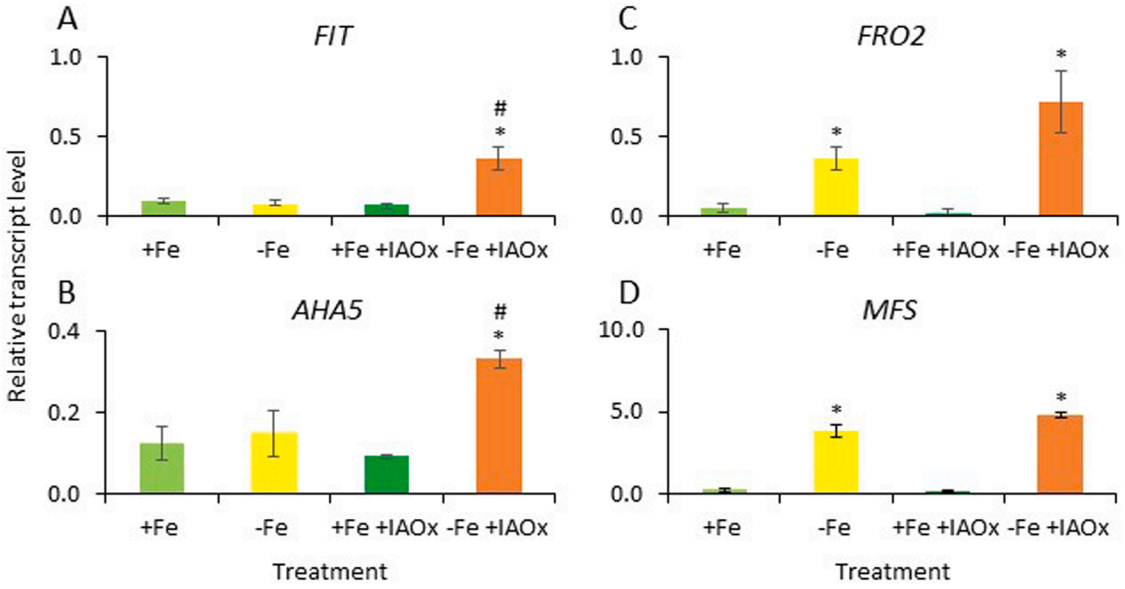

Fig. 7. Relative expression level of genes related to iron transport and reduction in roots and to flavin synthesis and secretion at day 7 after treatment (+Fe, -Fe, +Fe +IAOx, -Fe +IAOx). (A) *FIT* (transcription factor FER-LIKE IRON DEFICIENCY-INDUCED), (B) *AHA5* (plasma membrane H+-ATPase), (C) *FRO2* (Ferric reduction oxidase 2), (D) *MFS* (Hippocampus abundant transcript-like protein, major facilitator superfamily). Values represent mean ± SE of relative expression to reference genes *actin* (Actin-11) and *ProtS5A* (26S proteasome regulatory subunit S5A_2). Asterisks (*) indicate significant differences with respect to the control plants (+Fe) and hash symbols (#) differences between Fe-deficient plants treated with IAOx (-Fe +IAOx) with respect to deficient plants (-Fe) calculated using Student's test ($P < 0.05$).

(Fig. 3) and with literature (Ben Abdallah et al., 2017; Gheshlaghi et al., 2020). After 7 days of Fe starvation, genes involved in flavins biosynthesis and secretion followed a different trend. This indicates that flavins secreted to the hydroponic media are still essential to overcome Fe deficiency.

Altogether, *M. truncatula plants*, upon Fe starvation, exhibit the collection of symptoms and mechanisms that plants display to cope with Fe limitation.

Furthermore, a single dose of 100 μM of IAOx was able to induce the rooted phenotype observable from day 4 after treatment despite its important degradation in the nutrient solution at day 4. Plants treated with IAOx presented a decrease in the growth rate, total inhibition of the main root growth, and an increase in the number of lateral roots (Fig. 2), a phenotype similar to the previously nominated as "superroot phenotype" (Boerjan et al., 1995). Since there is an increase of secondary roots and root hairs which facilitates the nutrition of macro and micro-elements, we hypothesized that the phenotype-derived of the exogenous IAOx addition may have advantages to overcome nutritional stresses.

To our knowledge this is the first study evaluating the effect of the IAOx in hydroponically grown iron sufficient or deficient *Medicago* plants, therefore, changes are somehow unexpected. Thus, plants under both Fe-deficiency and IAOx treatments presented a phenotype similar to the Fe-sufficient plants treated with IAOx (Fig. 2). Surprisingly, plants under both treatments were less chlorotic than the Fe-deficient plants after 4 days upon treatment (Fig. 1). These plants delayed up to 3 days the pH decrease and the presence of flavins in root tips and nutrient solution compared to Fe-deficient plants (Fig. 3 A, E and F).

IAOx treatment delays the apparition of symptoms of Fe deficiency, which was consistent with the biochemical changes discussed above and in agreement with gene expression results. In other words, IAOx-treated Fe-deficient plants were insensitive to iron starvation at least to day 4 of Fe deficiency. In Fe-deficient plants treated with IAOx the expression of Fe deficiency related genes (*FIT, AHA5, FRO2, IRT1, bHLH39, GTPcII, DMRLs,* and *MFS)* was diminished with respect to Fe-deficient plants from day 2 or 4 (Fig. 6, Supp Table 1), but only the expression of *FIT* and *AHA5* was increased later, at day 7 (Fig. 7, Supp Table 1). As found here, the regulation of iron absorption is complex and time dependent, but molecular events respond to physiological demands. Thus, the involvement of membrane ATPase seems important in IAOx-treated Fe-deficient *Medicago* plants. There exist evidences supporting a modus operandi of auxin transporters where ATP hydrolysis favor auxin efflux and its cell-to-cell movement (Geisler, 2021).

As we stated above, we may speculate that the increase of secondary roots and the delay on Fe deficient symptoms after IAOx addition may produce a priming effect on the treated plants. Overall, the absence of symptoms of Fe deficiency in IAOx treated Fe-deficient plants can be explained by a putative signaling effect of IAOx or its subsequent metabolites that would be involved in the remobilization of Fe. In Arabidopsis under Fe-deficient conditions, it was observed that putrescine is involved in the remobilization of Fe from root cell wall hemicellulose in a process dependent on NO accumulation (Zhu et al., 2016). Moreover, it has been demonstrated in different species that NO acts downstream of auxins regulating lateral roots formation (García-Mina et al., 2013; Romera et al., 2011; Sun et al., 2017) while inhibiting root elongation by decreasing meristem activity in deficient root tips, with the involvement of auxin. In Arabidopsis the inhibition of primary roots is mediated by reducing acropetal auxin transport (Fernández-Marcos et al., 2011), suggesting that NO regulates root elongation based on the auxin levels in root tips. However, we cannot rule out that responses could be associated to a minor Fe requirement in Fe-deficient plants due to the smaller size of the IAOx treated plants as it was mentioned in other studies (Giehl and von Wirén, 2014).

IAOx has always been described as non-accumulated intermediate compound in the IAA pathway of non-Brassicaceae plants, but its presence has been proposed in maize (Irmisch et al., 2015) and in the legume *M. truncatula* (Buezo et al., 2019). Then, to explore it deeply we have determined in hydroponically grown *Medicago* plants the tryptophan derived molecules (IAOx, IAN, IAM, and IAA) contents in roots and shoots by HPLC-fluorescence. We found that endogenous IAOx accumulates in high amounts in roots and shoots at day 0, in similar amounts as found before in seedlings using this highly sensitive quantification

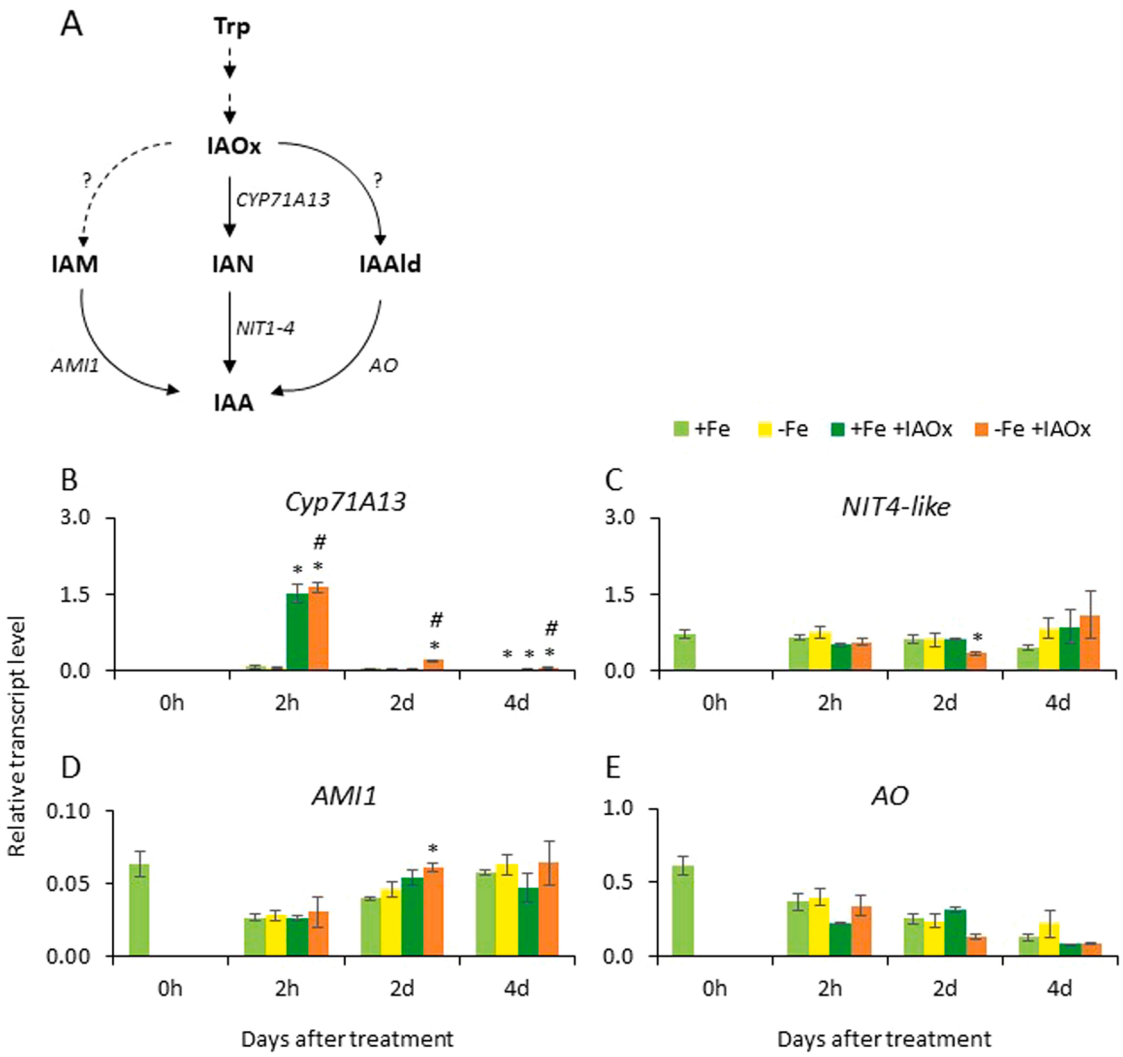

Fig. 8. Relative expression level of genes related to the IAA synthesis pathways in roots. (A). Simplified IAA synthesis pathway. (B, C, D, E) Time course (0 h, 2 h, 2 d and 4 d) after treatment application (+Fe, -Fe, +Fe +IAOx, -Fe +IAOx). (B) *Cyp71A13* (Cytochrome P450 family 71A13), (C) *NIT4-like* (Nitrilase/nitrile hydratase NIT4A-like protein), (D) *AMI1* (Amidase 1), (E) *AO* (Indole-3-acetaldehyde oxidase). Values represent mean ± SE of relative expression to reference genes *actin* (Actin-11) and *ProtS5A* (26S proteasome regulatory subunit S5A_2). Asterisks (*) indicate significant differences with respect to the control plants (+Fe) and hash symbols (#) differences between Fe-deficient plants treated with IAOx (-Fe +IAOx) with respect to Fe-deficient plants (-Fe) calculated using Student's test ($P < 0.05$). (adapted from Sanchez-Parra et al., 2014 and Olatunji et al., 2017).

technique (Buezo et al., 2019).

IAOx did not accumulate in shoots of Fe-sufficient plants after 4 days of IAOx addition but there was a high increase in shoots of Fe-deficient plants. Surprisingly, IAOx decreased in roots of both sufficient and deficient plants as found previously only in nitrogen-feed *Medicago* plants (Buezo et al., 2019). We may speculate that deficient plants transport efficiently IAOx to the aerial part and the translocation to maintain auxin homeostasis must be accurately regulated. Auxins are transported efficiently from where they are synthesized to the site where they are needed to modulate plant organ development (Brumos et al., 2018). Under Fe-deficiency conditions there exist evidences that polar transport of auxins increase in Arabidopsis (Yang et al., 2016). However, no specific IAOx transport mechanism has been described yet, neither basipetal or acropetal. Indeed, IAOx could be transported by IAA-related mechanisms polar or non-polar cell-to-cell, via eflux (PIN, ABCB) or influx (AUX) transporters (see Geisler and references therein for a review, 2021), thus, competing with IAA for the transporters or even for receptors. However, the latter scenario is still speculative since polar auxin transport is a black box for IAA and far from being understood (Geisler, 2021).

In IAOx treated plants, significant increases of IAN were found in shoots of sufficient and deficient plants and in roots of deficient plants. These data pointed out that IAOx, which accumulates in roots in Fe-deficient plants, is transformed to IAN or immediately transported to shoots and directly converted to IAN not only in deficient plants but also in sufficient plants, as proposed before (Buezo et al., 2019). In the same vein, in plants treated with IAOx, *Cyp71A*13 gene expression was highly induced after 2 h of treatment (Fig. 8 B, Supp Table 1), as it has been previously described in nitrogen-fed seedlings (Buezo et al., 2019), indicating that IAOx dehydratase rapidly dehydrates IAOx to IAN. Our results agree with the precedent research which suggests an active role of IAOx and the subsequent transformation. Fe-sufficient and deficient plants are processing IAOx to a non-metabolically active molecule, such as IAN, or transporting it to the shoot, to minimize the effect in roots.

In *Arabidopsis,* there is evidence that IAM is mainly generated from IAOx (Sugawara et al., 2009), and we hypothesize here that in *M. truncatula* this pathway could also exist. The rapid transformation of IAOx in roots produced an increase of IAM of Fe-sufficient plants and could explain why IAOx does not accumulate in shoots after exogenous oxime addition (Fig. 4). Unfortunately, we still do not have additional

candidate genes to monitor IAOx transformation except *CYP71A13* (Fig. 8 A) in this unknown and incomplete IAOx pathway. New knowledge on the genes encoding oxime-derived bioactive constituents as well as their transporters are expected to guide identification of missing genes to facilitate determination of the function of the products formed (Sørensen et al., 2018).

After exogenous IAOx addition, it has been described that the expression of *AO* seemed insensitive (Buezo et al., 2019), as we have confirmed in our results (Fig. 8 E). The expression of *NIT4-like* and *AMI1* were insensitive to IAOx addition too (Fig. 8 C-D). This is in agreement with no significant changes found in IAA levels after IAOx addition (Fig. 4), as previously described (Buezo et al., 2019). In hydroponic conditions we can conclude that rooted phenotype might be due to a direct effect of IAOx and not to IAA production.

Altogether, indolic compounds contents and gene expression in the IAOx pathway, indicates an alternative function for IAOx other than IAA synthesis. Based on our results, IAOx can alleviate the Fe deficiency in different ways. First, the synergistic phenotypical effect of IAOx that promotes an increase of the secondary roots in deficient treated plants, favor iron uptake. Additionally, IAOx or IAOx-derivatives can mimic an IAA-like compound, delaying Fe deficiency perception, although this novel hypothesis should be further explored in the future. IAOx is still a newly discovered compound in *M. truncatula*, and its role as a signaling molecule need further research to shed light into the action mechanism during Fe deficiency response in plants.

As a conclusion, IAOx play an active role in iron homeostasis delaying symptoms and responses in Fe-deficient *M. truncatula* plants. IAOx or its derivatives in a synergistic mechanism may well remobilize Fe from root cells to alleviate Fe-deficiency in the aerial part. It seems that IAOx pathway is tightly regulated in *M. truncatula* and IAOx compartmentation and translocation are essential to keep auxin transport and homeostasis.

Funding

This work was supported by the Spanish Research Agency [grant AGL2017-83358-R funded by MCIN/AEI/10.13039/501100011033 and by "ERDF A way of making Europe"] and the Government of Aragón [grant A09_23R], co-financed with FEDER funds; and the CSIC [grant 2020AEP119] to Y.G. This research was partially supported by [grants AGL2017-52396-P funded from MINECO (co-financed with FEDER funds) and PID-2020-1177 03GB-I00 from the Public University of Navarre] to J.F.M. J.M., M.U. and J.B. were the recipients of predoctoral contracts awarded by the Government of Aragon, Government of Navarre, and Public University of Navarre, Spain, respectively. A.R. was hired [grants AGL2017-83358-R and 2020AEP119]. We acknowledge support of the publication fee by the CSIC Gold Open Access Publication Support Initiative through its Unit of Information Resources for Research (URICI).

CRediT authorship contribution statement

A.R., J.F.M. and Y.G. devised the study objectives and designed the experiment. J.M., A.R. and L.F. performed the experiments, analysis of data and help to interpret the results. J.F.M. provided materials and supervised the research, M.U., A.C. and J.B. performed the analysis of indolic compounds and interpreted the results; A.C. performed the chemical synthesis of IAOx. A.R. drafted the manuscript. J.M., L.F., J.F. M. J.B. and M.U. contributed to review and edit the manuscript. Y.G. conceived the experiment, supervised the research, wrote and edit the manuscript, and provided funds. All authors read and approved the manuscript.

Declaration of Competing Interest

The authors declare that they have no known competing financial interests or personal relationships that could have appeared to influence the work reported in this paper.

Data Availability

Data will be made available on request.

Acknowledgment

We thank Dr. V. Martínez-Merino (INAMAT2-UPNA) to allow the use of its facilities for the chemical synthesis, and Drs J, Abadía, M.P. Vallés and A.M. Castillo (EEAD-CSIC) to allow the use of their equipments. In memorian of J. Abadía who taught us to love iron metabolism in plants and sadly passed away while this manuscript was almost finishing.

Appendix A. Supporting information

Supplementary data associated with this article can be found in the online version at doi:10.1016/j.plantsci.2023.111718.

References

J. Abadía, A. Álvarez-Fernández, M. Sanz, A. Abadía, A.D. Rombolà, M. Tagliavini, Technologies for the diagnosis and remediation of Fe deficiency, Soil Sci. Plant Nutr. 50 (2004) 965–971.

J. Abadía, A.F. López-Millán, A. Rombolà, A. Abadía, Organic acids and Fe deficiency: a review, Plant Soil 241 (2002) 75–86.

J. Abadía, S. Vázquez, R. Rellán-Álvarez, H. El-Jendoubi, A. Abadía, A. Álvarez-Fernández, A.F. López-Millán, Towards a knowledge-based correction of iron chlorosis, Plant Physiol. Biochem. 49 (2011) 471–482.

S. Andaluz, J. Rodríguez-Celma, A. Abadía, J. Abadía, A.-F. López-Millán, Time course induction of several key enzymes in *Medicago truncatula* roots in response to Fe deficiency, Plant Physiol. Biochem. 47 (2009) 1082–1088.

E. Bacaicoa, V. Mora, Á.M. Zamarreño, M. Fuentes, E. Casanova, J.M. García-Mina, Auxin: A major player in the shoot-to-root regulation of root Fe-stress physiological responses to Fe deficiency in cucumber plants, Plant Physiol. Biochem. 49 (2011) 545–556.

E. Bacaicoa, Á.M. Zamarreño, D. Leménager, R. Baigorri, J.M. García-Mina, Relationship between the hormonal balance and the regulation of iron deficiency stress responses in cucumber, J. Am. Soc. Hortic. Sci. 134 (2009) 589–601.

B. Bartel, G.R. Fink, Differential regulation of an auxin-producing nitrilase gene family in *Arabidopsis thaliana*, Proc. Natl. Acad. Sci. USA 91 (1994) 6649–6653.

H. Ben Abdallah, H.J. Mai, A. Álvarez-Fernández, J. Abadía, P. Bauer, Natural variation reveals contrasting abilities to cope with alkaline and saline soil among different *Medicago truncatula* genotypes, Plant Soil 418 (2017) 45–60.

W. Boerjan, M.T. Cervera, M. Delarue, T. Beeckman, W. Dewitte, C. Bellini, M. Caboche, H. Van Onckelen, M. Van Montagu, D. Inzé, Superroot, a recessive mutation in Arabidopsis, confers auxin overproduction, *Plant Cell* 7 (1995) 1405–1419.

J. Brumos, L.M. Robles, J. Yun, T.C. Vu, S. Jackson, J.M. Alonso, A.N. Stepanova, Local auxin biosynthesis is a key regulator of plant development, Dev. Cell 47 (2018) 306–318, e5.

J. Buezo, R. Esteban, A. Cornejo, P. López-Gómez, D. Marino, A. Chamizo-Ampudia, M. J. Gil, V. Martínez-Merino, J.F. Moran, IAOx induces the SUR phenotype and differential signalling from IAA under different types of nitrogen nutrition in *Medicago truncatula* roots, Plant Sci. 287 (2019), 110176.

J.L. Celenza, Metabolism of tyrosine and tryptophan - new genes for old pathways, Curr. Opin. Plant Biol. 4 (2001) 234–240.

W.W. Chen, J.L. Yang, C. Qin, C.W. Jin, J.H. Mo, T. Ye, S.J. Zheng, Nitric oxide acts downstream of auxin to trigger root ferric-chelate reductase activity in response to iron deficiency in Arabidopsis, Plant Physiol. 154 (2010) 810–819.

E.P. Colangelo, M.L. Guerinot, The essential basic helix-loop-helix protein FIT1 is required for the iron deficiency response, Plant Cell 16 (2004) 3400–3412.

I. Damiani, A. Drain, M. Guichard, S. Balzergue, A. Boscari, J.C. Boyer, V. Brunaud, S. Cottaz, C. Rancurel, M. da Rocha, et al., Nod factor effects on root hair-specific transcriptome of *Medicago truncatula*: Focus on plasma membrane transport systems and reactive oxygen species networks, Front. Plant Sci. 7 (2016) 794, https://doi.org/10.3389/fpls.2016.00794.

R. Esteban, B. Royo, E. Urarte, Á.M. Zamarreño, J.M. Garcia-Mina, J.F. Moran, Both free indole-3-acetic acid and photosynthetic performance are important players in the response of *Medicago truncatula* to urea and ammonium nutrition under axenic conditions, Front. Plant Sci. 7 (2016) 140, https://doi.org/10.3389/fpls.2016.00140.

M. Fernández-Marcos, L. Sanz, D.R. Lewis, G.K. Muday, O. Lorenzo, Nitric oxide causes root apical meristem defects and growth inhibition while reducing PIN-FORMED 1 (PIN1)-dependent acropetal auxin transport, Proc. Natl. Acad. Sci. U. S. A. 108 (2011) 18506–18511.

P. Fourcroy, P. Sisó-Terraza, D. Sudre, M. Savirón, G. Reyt, F. Gaymard, A. Abadía, J. Abadia, A. Álvarez-Fernández, J.F. Briat, Involvement of the ABCG37 transporter

in secretion of scopoletin and derivatives by *Arabidopsis* roots in response to iron deficiency, N. Phytol. 201 (2014) 155–167.
T.C. Fox, M.L. Guerinot, Molecular biology of cation transport in plants, Annu. Rev. Plant Physiol. Plant Mol. Biol. 49 (1998) 669–696.
J.M. García-Mina, E. Bacaicoa, M. Fuentes, E. Casanova, Fine regulation of leaf iron use efficiency and iron root uptake under limited iron bioavailability, Plant Sci. 198 (2013) 39–45.
M.M. Geisler, A retro-perspective on auxin transport, Front. Plant Sci. 12 (2021), 756968, https://doi.org/10.3389/fpls.2021.756968.
Z. Gheshlaghi, Adrián Luis-Villarroya, A. Álvarez-Fernández, R. Khorassani, J. Abadía, Iron deficient *Medicago scutellata* grown in nutrient solution at high pH accumulates and secretes large amounts of flavins, Plant Sci. 303 (2020), 110664, https://doi.org/10.1016/j.plantsci.2020.110664.
R.F.H. Giehl, N. von Wirén, Root nutrient foraging, Plant Physiol. 166 (2014) 509–517.
Y. Gogorcena, J. Abadía, A. Abadía, Induction of in vivo root ferric chelate reductase activity in fruit tree rootstock, J. Plant Nutr. 23 (2000) 9–21.
M. Graziano, L. Lamattina, Nitric oxide accumulation is required for molecular and physiological responses to iron deficiency in tomato roots, Plant J. 52 (2007) 949–960.
M.N. Hindt, M.L. Guerinot, Getting a sense for signals: Regulation of the plant iron deficiency response, Biochim. Biophys. Acta - Mol. Cell Res. 1823 (2012) 1521–1530.
S. Irmisch, P. Zeltner, V. Handrick, J. Gershenzon, T.G. Köllner, The maize cytochrome P450 CYP79A61 produces phenylacetaldoxime and indole-3-acetaldoxime in heterologous systems and might contribute to plant defense and auxin formation, BMC Plant Biol. 15 (2015) 128, https://doi.org/10.1186/s12870-015-0526-1.
S. Jiménez, J. Pinochet, A. Abadía, M.Á. Moreno, Y. Gogorcena, Tolerance response to iron chlorosis of *Prunus* selections as rootstocks, Hort. Sci. 43 (2008) 304–309.
C.W. Jin, S.T. Du, I.H. Shamsi, B.F. Luo, X.Y. Lin, NO synthase-generated NO acts downstream of auxin in regulating Fe-deficiency-induced root branching that enhances Fe-deficiency tolerance in tomato plants, J. Exp. Bot. 62 (2011) 3875–3884.
C.W. Jin, Y.F. He, C.X. Tang, P. Wu, S.J. Zheng,) Mechanisms of microbially enhanced Fe acquisition in red clover (*Trifolium pratense L.*), Plant. Cell Environ. 29 (2006) 888–897.
C.W. Jin, G.Y. You, Y.F. He, C. Tang, P. Wu, S.J. Zheng, Iron deficiency-induced secretion of phenolics facilitates the reutilization of root apoplastic iron in red clover, Plant Physiol. 144 (2007) 278–285.
V. Kriechbaumer, W.J. Park, M. Piotrowski, R.B. Meeley, A. Gierl, E. Glawischnig, Maize nitrilases have a dual role in auxin homeostasis and β-cyanoalanine hydrolysis, J. Exp. Bot. 58 (2007) 4225–4233.
E. Larrainzar, B.K. Riely, S.C. Kim, N. Carrasquilla-Garcia, H.J. Yu, H.J. Hwang, M. Oh, G.B. Kim, A.K. Surendrarao, D. Chasman, et al., Deep sequencing of the *Medicago truncatula* root transcriptome reveals a massive and early interaction between nodulation factor and ethylene signals. Plant Physiol. 169 (2015) 233–265.
T. Lehmann, M. Hoffmann, M. Hentrich, S. Pollmann, Indole-3-acetamide-dependent auxin biosynthesis: a widely distributed way of indole-3-acetic acid production? Eur. J. Cell Biol. 89 (2010) 895–905.
G.J. Lei, X.F. Zhu, Z.W. Wang, F. Dong, N.Y. Dong, S.J. Zheng, Abscisic acid alleviates iron deficiency by promoting root iron reutilization and transport from root to shoot in *Arabidopsis*, Plant, Cell Environ. 37 (2014) 852–863.
G. Li, B. Wang, Q. Tian, T. Wang, W.H. Zhang, *Medicago truncatula* ecotypes A17 and R108 differed in their response to iron deficiency, J. Plant Physiol. 171 (2014) 639–647.
H. Li, L. Wang, Z.M. Yang, Co-expression analysis reveals a group of genes potentially involved in regulation of plant response to iron-deficiency, Gene 554 (2015) 16–24.
W. Li, W. Schmidt, A lysine-63-linked ubiquitin chain-forming conjugase, UBC13, promotes the developmental responses to iron deficiency in Arabidopsis roots, Plant J. 62 (2010) 330–343.
W.L. Lindsay, A.P. Schwab, The chemistry of iron in soils and its availability to plants, J. Plant Nutr. 5 (1982) 821–840.
A.F. López-Millán, F. Morales, S. Andaluz, Y. Gogorcena, A. Abadía, J. De Las Rivas, J. Abadia, Responses of sugar beet roots to iron deficiency, Chang. Carbon Assim. Oxyg. Use *Plant Physiol.* 124 (2000) 885–897.
C. Lucena, F.J. Romera, M.J. García, E. Alcántara, R. Pérez-Vicente, Ethylene participates in the regulation of Fe deficiency responses in strategy I plants and in rice, Front. Plant Sci. 6 (2015) 1056, https://doi.org/10.3389/fpls.2015.01056.
Y. Mano, K. Nemoto, The pathway of auxin biosynthesis in plants, J. Exp. Bot. 63 (2012) 2853–2872.
V. Montejano-Ramírez, E. García-Pineda, E. Valencia-Cantero, Bacterial compound n,n-dimethylhexadecylamine modulates expression of iron deficiency and defense response genes in *Medicago truncatula* independently of the jasmonic acid pathway, Plants 9 (2020) 624, https://doi.org/10.3390/plants9050624.
P.R. Moog, W. Brüggemann, Iron reductase systems on the plant plasma membrane-a review, Plant Soil 165 (1994) 241–260.
M. Müller, W. Schmidt, Environmentally induced plasticity of root hair development in Arabidopsis, Plant Physiol. 134 (2004) 409–419.
M. Nafisi, S. Goregaoker, C.J. Botanga, E. Glawischnig, C.E. Olsen, B.A. Halkier, J. Glazebrook, *Arabidopsis* cytochrome P450 monooxygenase 71A13 catalyzes the conversion of indole-3-acetaldoxime in camalexin synthesis, Plant Cell 19 (2007) 2039–2052.
D. Olatunji, D. Geelen, I. Verstraeten, Control of endogenous auxin levels in plant root development, Int. J. Mol. Sci. 18 (12) (2017) 2587, https://doi.org/10.3390/ijms18122587.
M.M. Pérez-Alonso, B. Sánchez-Parra, P. Ortiz-García, M.E. Santamaría, I. Díaz, S. Pollmann, Jasmonic acid-dependent myc transcription factors bind to a tandem g-box motif in the yucca8 and yucca9 promoters to regulate biotic stress responses, Int. J. Mol. Sci. 22 (18) (2021) 9768, https://doi.org/10.3390/ijms22189768.
G.S. Pound, G.W. Welkie, Iron nutrition of Nicotiana tabacum L. in relation to multiplication of tobacco mosaic virus, Virology 5 (1958) 371–381.
R. Rajagopal, P. Larsen, Metabolism of indole-3-acetaldoxime in plants, Planta 103 (1972) 45–54.
J. Rodríguez-Celma, G. Lattanzio, M.A. Grusak, J. Abadía, Root responses of *Medicago truncatula* plants grown in two different iron deficiency conditions: Changes in root protein profile and riboflavin biosynthesis, J. Proteome Res. 10 (2011) 2590–2601.
J. Rodríguez-Celma, W. Lin, G. Fu, J. Abadía, W. Schmidt, Mutually exclusive alterations in secondary metabolism are critical for the uptake of insoluble iron compounds by Arabidopsis and *Medicago truncatula*, Plant Physiol. 162 (2013) 1473–1485.
F.J. Romera, E. Alcántara, Iron-deficiency stress responses in cucumber, Plant Physiol. 105 (1994) 1133–1138.
F.J. Romera, M.J. García, E. Alcántara, R. Pérez-Vicente, Latest findings about the interplay of auxin, ethylene and nitric oxide in the regulation of Fe deficiency responses by Strategy I plants, Plant Signal. Behav. 6 (2011) 167–170.
J.M. Ruijter, C. Ramakers, W.M.H. Hoogaars, Y. Karlen, O. Bakker, M.J.B. van den Hoff, A.F.M. Moorman, Amplification efficiency: linking baseline and bias in the analysis of quantitative PCR data, Nucleic Acids Res 37 (6) (2009), e45, https://doi.org/10.1093/nar/gkp045.
B. Sánchez-Parra, H. Frerigmann, M.M.P. Alonso, V.C. Loba, R. Jost, M. Hentrich, S. Pollmann, Characterization of four bifunctional plant IAM/PAM-amidohydrolases capable of contributing to auxin biosynthesis, Plants 3 (2014) 324–347.
S. Santi, W. Schmidt, Dissecting iron deficiency-induced proton extrusion in Arabidopsis roots, N. Phytol. 183 (2009) 1072–1084.
W. Schmidt, Mechanisms and regulation of reduction-based iron uptake in plants, N. Phytol. 141 (1999) 1–26.
B. Schwarz, C.B. Azodi, S.H. Shiu, P. Bauer, Putative cis-regulatory elements predict iron deficiency responses in Arabidopsis roots, Plant Physiol. 182 (2020) 1420–1439.
M. Séguéla, J.F. Briat, G. Vert, C. Curie, Cytokinins negatively regulate the root iron uptake machinery in Arabidopsis through a growth-dependent pathway, Plant J. 55 (2008) 289–300.
P. Sisó-Terraza, J.J. Rios, J. Abadía, A. Abadía, A. Alvarez-Fernández, Flavins secreted by roots of iron-deficient *Beta vulgaris* enable mining of ferric oxide via reductive mechanisms, N. Phytol. 209 (2016) 733–745.
M. Sørensen, E.H.J. Neilson, B.L. Møller, Oximes: Unrecognized chameleons in general and specialized plant metabolism, Mol. Plant 11 (2018) 95–117.
Sugawara, S., Hishiyama, S., Jikumaru, Y., Hanada, A., Nishimura, T., Koshiba, T., Zhao, Y., Kamiya, Y. and Kasahara, H. (2009) Biochemical analyses of indole-3-acetaldoxime dependent auxin biosynthesis in Arabidopsis. Proc. Natl. Acad. Sci. U. S.A., 106, 5430–5435.
H. Sun, F. Feng, J. Liu, Q. Zhao, The interaction between auxin and nitric oxide regulates root growth in response to iron deficiency in rice, Front. Plant Sci. 8 (2017) 1–14.
S. Susín, J. Abián, F. Sánchez-Baeza, M.L. Peleato, A. Abadía, E. Gelpí, J. Abadía, Riboflavin 3′- and 5′-sulfate, two novel flavins accumulating in the roots of iron-deficient sugar beet (*Beta vulgaris*), J. Biol. Chem. 268 (1993) 20958–20965.
N.D. Tivendale, J.J. Ross, J.D. Cohen, The shifting paradigms of auxin biosynthesis, Trends Plant Sci. 19 (2014) 44–51.
H.H. Tsai, W. Schmidt, pH-dependent transcriptional profile changes in iron-deficient *Arabidopsis* roots, BMC Genom. 21 (2020) 694, https://doi.org/10.1186/s12864-020-07116-6.
J. Vandesompele, K. Preter, De, F. Pattyn, B. Poppe, N. Roy, Van, A. Paepe, De, F. Speleman, Accurate normalization of real-time quantitative RT-PCR data by geometric averaging of multiple internal control genes, *Genome Biol.*, 3 (7), research0034 1–0034 (2002) 11, https://doi.org/10.1186/gb-2002-3-7-research0034.
A. Vorwieger, C. Gryczka, A. Czihal, D. Douchkov, J. Tiedemann, H.P. Mock, M. Jakoby, B. Weisshaar, I. Saalbach, H. Bäumlein, Iron assimilation and transcription factor controlled synthesis of riboflavin in plants, Planta 226 (2007) 147–158.
Y. Wang, W. Yang, Y. Zuo, L. Zhu, A.H. Hastwell, L. Chen, Y. Tian, C. Su, B.J. Ferguson, X. Li, GmYUC2a mediates auxin biosynthesis during root development and nodulation in soybean, J. Exp. Bot. 70 (2019) 3167–3176.
L.H. Weinstein, E.R. Purvis, A.N. Meiss, R.L. Uhler, Chelates, absorption and translocation of ethylenediaminetetraacetic acid by sunflower plants, J. Agric. Food Chem. 2 (1954) 421–424.
M. Wild, J. Davie, T. Regnault, G. Dubeaux, T. Regnault, L. Sakvarelidze-Achard, E. Carrera, Tissue-specific regulation of gibberellin signaling article tissue-specific regulation of gibberellin signaling fine-tunes *Arabidopsis* iron-deficiency responses, Dev. Cell 37 (2016) 190–200.
L. Yang, J. Ji, H. Wang, K.R. Harris-Shultz, E.F. Abd_Allah, Y. Luo, Y. Guan, X. Hu, Carbon monoxide interacts with auxin and nitric oxide to cope with iron deficiency in *Arabidopsis*, Front. Plant Sci. 7 (2016) 112, https://doi.org/10.3389/fpls.2016.00112.
M. Yu, L. Lamattina, S.H. Spoel, G.J. Loake, Nitric oxide function in plant biology: a redox cue in deconvolution, N. Phytol. 202 (2014) 1142–1156.
Y. Yuan, H. Wu, N. Wang, J. Li, W. Zhao, J. Du, D. Wang, H.-Q. Ling, FIT interacts with AtbHLH38 and AtbHLH39 in regulating iron uptake gene expression for iron homeostasis in *Arabidopsis*, Cell Res 18 (2008) 385–397.
X.F. Zhu, B. Wang, W.F. Song, S.J. Zheng, R.F. Shen, Putrescine alleviates iron deficiency via NO-dependent reutilization of root cell-wall fe in Arabidopsis, Plant Physiol. 170 (2016) 558–567.